Analysis of the Substrate Specificity of the *Staphylococcus aureus* Sortase Transpeptidase SrtA†

Ryan G. Kruger, Balint Otvos, Brenda A. Frankel, Matthew Bentley, Patrick Dostal, and Dewey G. McCafferty*

Johnson Research Foundation and Department of Biochemistry and Biophysics, The University of Pennsylvania School of Medicine, Philadelphia, Pennsylvania 19104-6059

Received October 28, 2003; Revised Manuscript Received November 25, 2003

ABSTRACT: The *Staphylococcus aureus* sortase transpeptidase SrtA isoform is responsible for the covalent attachment of virulence and colonization-associated proteins to the bacterial peptidoglycan. SrtA utilizes two substrates, undecaprenol-pyrophosphoryl-MurNAc(GlcNAc)-Ala-D-*iso*Glu-Lys(ϵ-Gly_5)-D-Ala-D-Ala (branched Lipid II) and secreted proteins containing a highly conserved C-terminal LPXTG sequence. SrtA simultaneously cleaves the Thr−Gly bond of the LPXTG-containing protein and forms a new amide bond with the nucleophilic amino group of the Gly_5 portion of branched Lipid II, anchoring the protein to this key intermediate that is subsequently polymerized into peptidoglycan. Here we describe the development of a general *in vitro* method for elucidating the substrate specificity of sortase enzymes. In addition, using immunofluorescence, cell adhesion assays, and transmission electron microscopy, we establish links between *in vitro* substrate specificity and *in vivo* function of the *S. aureus* sortase isoforms. Results from these studies provide strong supporting evidence of a primary role of the SrtA isoform in *S. aureus* adhesion and host colonization, illustrate a lack of specificity cross talk between SrtA and SrtB isoforms, and highlight the potential of SrtA as a target for the development of antivirulence chemotherapeutics against Gram-positive bacterial pathogens.

During pathogenesis, Gram-positive bacteria utilize surface protein virulence factors such as the MSCRAMMs (microbial surface components recognizing adhesive matrix molecules) to aid the initiation and propagation of infection through adherence to host endothelial tissue and immune system evasion (*1*, *2*). These virulence-associated proteins are covalently anchored to bacterial cell wall peptidoglycan through a general sorting mechanism catalyzed by a superfamily of membrane-associated transpeptidases termed *sortases* (*1*).

A host of genetic evidence supports the identification of sortase transpeptidases as functionally important enzymes in virulence and infection processes. For example, SrtA null *Staphylococcus aureus* mutants fail to anchor LPXTG-containing proteins and are unable to form renal abscesses in a mouse model of infection (*3*). Inactivation of SrtA in *Streptococcus gordonii* resulted in a decreased ability of the bacteria to bind fibronectin as well as inhibition of bacterial colonization in the oral cavity of mice (*4*). SrtA deficient *Listeria monocytogenes* exhibited a decreased ability to display internalin and were less invasive *in vitro*, and mice injected with a lethal dose of these bacteria were able to fully recover (*5*). In a similar study, *L. monocytogenes* containing an inactivated SrtA were unable to colonize the liver and spleen of mice (*6*). Together, these studies provide very strong evidence that the sortase enzymes are important antivirulence targets.

Among Gram-positive bacteria, multiple sortase isoforms are typically found within a single species. For example, the *S. aureus* genome encodes two sortase homologues, and in *Streptomyces coelicolor*, seven potential sortase isoforms have been identified (*7*). Although the roles of these different isoforms remain unclear, there is a growing body of evidence which suggests that different isoforms likely are responsible for specific physiological roles by anchoring specific subsets of surface proteins. For example, Barnett and colleagues have shown that there are two sortase isoforms in *Streptococcus pyogenes*, one of which anchors protein F and the M6, ScpA, and GRAB virulence proteins, while the other is specific for cell wall attachment of T6, a protein of unknown function (*8*). In another study, Osaki and co-workers have shown that while the *srtA* gene is strongly divergent among 59 strains of *Streptococcus suis*, the function of this particular isoform, one of five present in *S. suis*, has been conserved. This suggests that the loss of function of the *S. suis* SrtA cannot be offset by the presence of the other four isoforms (*9*). Collectively, these studies indicate discreet functional roles for sortase isoforms within a bacterium in both cell wall protein anchoring and other less obvious physiological phenomena.

In *S. aureus*, two sortase isoforms have been identified, SrtA and SrtB. The SrtA isoform utilizes two substrates, undecaprenol-pyrophosphoryl-MurNAc(GlcNAc)-Ala-D-*iso*-

† This work was generously supported by grants from the National Institutes of Health (AI46611 and GM65539), the American Cancer Society (RPG-99-312-01), the McCabe Fund, and the University of Pennsylvania Research Foundation. B.A.F. is the recipient of an NSF predoctoral fellowship.

* To whom correspondence should be addressed: Department of Biochemistry and Biophysics, The University of Pennsylvania School of Medicine, 905A Stellar-Chance Building, 422 Curie Blvd., Philadelphia, PA 19104-6059. Phone: (215) 898-7619. Fax: (215) 573-8052. E-mail: deweym@mail.med.upenn.edu.

10.1021/bi035920j CCC: $27.50
Published on Web 01/24/2004

Glu-Lys(ϵ-Gly_5)-D-Ala-D-Ala (branched Lipid II) and secreted proteins containing a tripartite recognition motif that includes a highly conserved C-terminal LPXTG sequence followed by a region containing predominantly hydrophobic residues terminating with several basic residues (*10*, *11*). The latter two regions purportedly serve to help lock the protein substrate in the membrane prior to cell wall anchoring. SrtA catalyzes the cleavage of the Thr−Gly bond of the LPXTG-containing proteins as well as the concomitant formation of a new amide bond with the nucleophilic amino group of the Gly_5 portion of branched Lipid II, thus covalently attaching the protein by transpeptidation to this key cell wall biosynthetic intermediate. Once acylated, branched Lipid II is subsequently polymerized into mature peptidoglycan, anchoring the LPXTG-containing protein to the outer surface of the *S. aureus* cell wall (*12*, *13*).

Similarly, preliminary studies of the *S. aureus* sortase isoform SrtB have shown that the gene is found within an operon devoted to heme iron uptake, and thus, its expression is tightly regulated under control of a ferric iron uptake promoter (*fur* promoter) (*14*, *15*). Schneewind and colleagues have demonstrated that SrtB is responsible for the attachment of an NPQTN-containing protein (IsdC) to the *S. aureus* cell wall by a mechanism qualitatively similar to that of SrtA, albeit the exact structure of the covalent link to the cell wall has not yet been elucidated (*14*, *15*).

While the LPXTG motif is highly conserved among all Gram-positive bacteria and the NPQTN motif appears to be conserved only among at least three bacteria containing the heme iron acquisition *isd* gene locus (*Bacillus anthracis*, *Bacillus halodurans*, and *S. aureus*), predicted and actual sortase substrates possess significant amino acid variants within each position of the respective pentapeptide motifs (*1*, *7*, *10*, *16*, *17*). Because numerous potential LPXTG-containing sortase substrates exist, and within many Gram-positive bacterial pathogens multiple sortase isoforms are found, assigning a discreet physiological function to a single isoform has proven to be challenging. To address this long-term goal, we describe here the application of a general *in vitro* method for the evaluation of the substrate specificity of the *S. aureus* sortase isoform SrtA. We also establish firm links between *in vitro* substrate specificity preference and *in vivo* function of the two staphylococcal SrtA and SrtB isoforms. Results from these studies provide strong supporting evidence of a primary role of the SrtA isoform in bacterial adhesion and host colonization events and furthermore illustrate the potential of SrtA as an antivirulence target for staphylococcal infections.

EXPERIMENTAL PROCEDURES

Materials and Reagents. Buffer salts were purchased from Sigma. pUC19 and pET15b vectors were purchased from Gibco and Novagen, respectively. *Escherichia coli* DH5α subcloning competent cells (Invitrogen) and *E. coli* BL21(DE3) electrocompetent cells (Novagen) were used according to the manufacturers' recommendations. QIAEXII gel extraction and QIAprep spin miniprep DNA purification kits were purchased from Qiagen. Restriction enzymes and T4 DNA ligase were obtained from New England Biolabs. Amicon stirred ultrafiltration cells and membranes were purchased from Millipore. DNA sequencing was performed by the University of Pennsylvania Genetics Core Facility. Standard Fmoc amino acids (Novabiochem), Fmoc-Dap(Dnp)-OH[1] (Bachem), Fmoc-Lys(Dde)-OH (Bachem), NH_2-Gly_5-OH (Bachem), and Dnp-Ala-OH (Sigma) were purchased and used without further purification. 5-(4-Fmoc-Aminomethyl-3,5-dimethoxyphenoxy)valeric acid-MBHA (PAL) resin (Advanced Chemtech) was used for solid-phase peptide synthesis. *S. aureus* genomic DNA was a kind gift from G. Wright (McMaster University, Hamilton, ON). *S. aureus* Newman, $SrtA^-$ (SKM12), $SrtB^-$ (SKM7), and $SrtA^-/SrtB^-$ (SKM14) strains were generously provided by O. Schneewind (University of Chicago, Chicago, IL) (*18*). Fibronectin-coated 96-well microtiter plates were purchased from Biocoat Cell Environments. Cy3-labeled IgG was purchased from Jackson ImmunoResearch Laboratories, Inc. Protein purification was performed on a Biocad Sprint chromatography system (Applied Biosystems). Chelating Sepharose fast flow chromatography resin (Pharmacia Biotech) and a HiPrep 26/60 Sephacryl S-200 high-resolution gel filtration column (Pharmacia Biotech) were used according to the manufacturers' recommendations. Solid-phase peptide synthesis was performed on either an automated 433A synthesizer (Applied Biosystems) or an Argonaut Quest parallel synthesizer equipped with an automated solvent delivery system. All mass spectrometry data were obtained on a Voyager MALDI-TOF spectrometer (Applied Biosystems). HPLC was performed using a Thermo Separation Products SpectraSYSTEM equipped with an autosampler and either a semipreparative Jupiter octadecyl silica column (Phenomenex) or an analytical (4.6 mm × 250 mm, 5 μm) or fast analytical (4.6 mm × 50 mm, 3 μm) octadecyl silica column (Vydac).

Cloning of S. aureus $SrtA_{\Delta N24}$. Routine molecular biology techniques were performed as described in *Molecular Cloning: A Laboratory Manual*, 2nd ed. (*19*). Primer pairs $SrtA_{\Delta N24}$fwd (5′-CCCGAATTCCATATGAAACCACATATC-GATAATTATCTTCAC-3′) and $SrtA_{\Delta N24}$rvrs (5′-CATT-AGCGTGGATCCCTCGAGTTATTTGACTTCTGTAGC-TACAAA-3′) were used to PCR amplify $SrtA_{\Delta N24}$ from *S. aureus* genomic DNA. Both resulting DNA fragments were doubly digested with *Eco*RI and *Bam*HI and individually ligated with T4 DNA ligase into a pUC19 cloning vector previously treated with *Eco*RI and *Bam*HI to generate plasmid pUC19$SrtA_{\Delta N24}$. These plasmids were subsequently transformed into *E. coli* DH5α cells, isolated with a QIAprep spin miniprep kit, and confirmed for the desired sequence by DNA sequencing. Both plasmids were subsequently digested with *Bam*HI and *Nde*I to liberate the desired gene and subcloned into a similarly treated pET15b expression vector to generate the pET15b$SrtA_{\Delta N24}$ plasmids. The plasmid was subsequently transformed into *E. coli* BL21(DE3) cells for protein expression.

Overproduction and Purification of His_6-Tagged S. aureus $SrtA_{\Delta N24}$. An overnight culture (40 mL) of *E. coli* BL21-(DE3) harboring the pET15b$SrtA_{\Delta N24}$ plasmid was used to inoculate flasks of Luria Broth (LB, 2 L) containing

[1] Abbreviations: Dap, diaminopropionic acid; Dnp, 2,4-dinitrophenyl; Abz, anthranilic acid; HPLC, high-performance liquid chromatography; MALDI-TOF MS, matrix-assisted laser desorption ionization time-of-flight mass spectroscopy; MN, *N*-acetylmuramylglucosamine; GN, *N*-acetylglucosamine; TFA, trifluoroacetic acid; TIS, triisopropylsilane; Fmoc, 9-fluorenylmethoxycarbonyl.

ampicillin (100 μg/mL). Cultures were grown in baffled flasks with agitation at 37 °C to an OD_{580} of 0.8. IPTG (1 mM) was subsequently added to initiate expression, and after 3 h, the cells were harvested by centrifugation (3000*g* for 10 min) and then flash-frozen at −80 °C. Pellets could then be stored at −80 °C for at least 12 months with no appreciable protein degradation. Pellets were thawed on ice and suspended in buffer A [150 mM NaCl, 50 mM Tris, 5 mM imidazole, and 10% glycerol (pH 7.5)]. Bacteria were lysed three times with a French pressure cell (14 000 psi); the lysate was centrifuged (150000*g* for 1 h), and the extract was applied to a chelating Sepharose fast flow column (10 mL, 1 mL/min) previously charged with $NiSO_4$ and equilibrated with buffer A. The column was washed with 100 mL of buffer A (1 mL/min), and then the desired protein was eluted using a linear gradient from 5 to 500 mM imidazole over the course of 1 h. Fractions containing $SrtA_{\Delta N24}$ as determined by SDS−PAGE analysis were pooled and concentrated to 5 mL using 10 kDa molecular mass Centriprep concentrators. Concentrated protein was loaded onto a HiPrep 26/60 Sephacryl S-200 gel filtration column (1 mL/min) that was pre-equilibrated with buffer B [150 mM NaCl, 50 mM Tris, 5 mM $CaCl_2$, 0.1% β-mercaptoethanol, and 10% glycerol (pH 7.5)]. Fractions containing $SrtA_{\Delta N24}$ as determined by SDS−PAGE analysis were pooled and concentrated to 200 μM with an Amicon stirred ultrafiltration cell fitted with a 10 kDa molecular mass membrane. The protein concentration of the purified enzyme was determined by the von Hippel method ($\epsilon_{280} = 17\,420\ M^{-1}\ cm^{-1}$) (*20*, *21*). Enzyme aliquots (100 μL) were frozen on dry ice and stored at −80 °C. Samples of the protein (100 μL) were taken after cell lysis, nickel chromatography, and gel filtration chromatography steps for activity and purity analysis. Protein concentrations of partially purified samples were determined using the Bradford method using bovine serum albumin (BSA) as a standard (*22*).

Solid-Phase Synthesis of Sortase Substrates. Peptide substrates for sortase activity assays were synthesized by the Fmoc/piperidine strategy on PAL resin on a 0.25 mmol scale using an Applied Biosystems 433A synthesizer. Peptides were cleaved using a 95:5 TFA/water mixture for 3 h. Excess TFA was removed by rotary evaporation, and the peptides were precipitated using cold diethyl ether, filtered with a fine porosity fritted glass filter, dissolved in water, and lyophilized to afford the desired crude peptide products. All peptides were purified by HPLC using a preparative C_{18} Jupiter column to ≥98% purity and analyzed by MALDI-TOF MS. Purified peptides were lyophilized and stored at −20 °C.

HPLC Analysis of $SrtA_{\Delta N24}$ Activity. Transpeptidation assays were carried out in 100 μL reaction mixtures containing buffer C [150 mM NaCl, 300 mM Tris, and 5 mM $CaCl_2$ (pH 7.5)], pentaglycine (2 mM), $SrtA_{\Delta N24}$ (840 nM), and varying concentrations of Abz-LPETG-Dap(Dnp)-NH_2 (from 0 to 10 mM). Reactions were initiated by the addition of enzyme; mixtures were incubated at 37 °C for 30 min, and 50 μL aliquots were removed and reactions quenched by the addition of 1 N HCl (25 μL). The reaction mixtures were injected directly onto a Vydac reversed-phase C_{18} fast analytical HPLC column, and the peptides were separated using a 10 to 40% linear gradient with a CH_3CN/0.1% TFA mixture over the course of 5 min. Dnp-containing peaks were detected by absorbance at 355 nm, and the peak area was converted to concentration units using a calibration curve of Abz-LPETG-Dap(Dnp)-NH_2 as the standard. To confirm the composition and identity of each product, the peaks were collected and analyzed by MALDI-TOF MS. Similar assays using Dnp-AQALPETGEE-NH_2 were also performed with the exception being the HPLC separation protocol. Dnp-AQALPETGEE-NH_2-containing reaction mixtures were injected directly onto a Vydac reversed-phase C_{18} analytical HPLC column, and the peptides were separated isocratically in a 20% CH_3CN/0.1% TFA mixture over the course of 40 min.

Solid-Phase Synthesis of Substrate Libraries. The Dnp-A$\underline{X}$PETG-NH_2, Dnp-AL$\underline{X}$ETG-NH_2, Dnp-ALP$\underline{X}$TG-NH_2, Dnp-ALPE$\underline{X}$G-NH_2, and Dnp-ALPET$\underline{X}$-NH_2 peptide libraries were synthesized in parallel by the Fmoc/piperidine strategy on PAL resin on a 0.1 mmol scale using an Argonaut Quest parallel synthesizer, where X represents each of the natural amino acids, excluding cysteine and tryptophan. Peptides were cleaved using a 95:2.5:2.5 TFA/TIS/water mixture for 3 h. To facilitate purification in parallel, a solid-phase extraction vacuum manifold was used to perform the following steps. Excess TFA was evaporated by passing dry air over the crude peptides. The peptides were then precipitated with cold diethyl ether, filtered with a fine porosity filter, and dissolved in methanol. The crude peptides were then loaded onto C_{18} solid-phase extraction columns pre-equilibrated with 99.9% water and 0.1% TFA. The columns were washed with a 2:8 CH_3CN/water mixture and eluted with a 1:1 CH_3CN/water mixture. The partially purified peptides were lyophilized and stored at −20 °C. The purity of each member of the library was assessed by analytical HPLC, and all were found to be ≥80% pure. Additional purification was performed as needed by HPLC. Peptide masses of the library members were confirmed by MALDI-TOF MS.

HPLC Screening of Substrate Libraries by $SrtA_{\Delta N24}$. Transpeptidation assays of the Dnp-A$\underline{X}$PETG-NH_2, Dnp-AL$\underline{X}$ETG-NH_2, Dnp-ALP$\underline{X}$TG-NH_2, Dnp-ALPE$\underline{X}$G-NH_2, and Dnp-ALPET$\underline{X}$-NH_2 libraries were performed in 100 μL reaction mixtures containing buffer C, $SrtA_{\Delta N24}$ (15 μM), Gly_5 (2 mM), and peptide (300 μM). Reactions were initiated by the addition of enzyme, incubated at 37 °C for 30 min, and quenched by the addition of 1 N HCl (50 μL). The reaction mixtures were injected directly onto a Vydac reversed-phase C_{18} fast analytical HPLC column, and the peptides were separated using one of three gradients. Substrate and product peaks were detected by absorbance at 355 nm, and the amount of product formed was calculated for each substrate in the library. Reaction mixtures containing Dnp-ALPHTG-NH_2, Dnp-ALPRTG-NH_2, and Dnp-ALPKTG-NH_2 were not resolved, but progress was confirmed by MALDI-TOF MS analysis. To increase the sensitivity of the assay to identify more substrates that can be utilized by SrtA, these assays were repeated using 60 μM $SrtA_{\Delta N24}$ for 360 min.

In Silico Prediction of Sortase Substrates. Nine microbial genomes with complete sequences (http://www.tigr.org) were searched for open reading frames encoding potential protein substrates for the sortase enzyme using a modification of the method of Masmussen (*11*) (*S. aureus* strains N315, Mu50, COL, and MW2, *Enterococcus faecalis* V583, *L.*

Table 1: Purification of $SrtA_{\Delta N24}$

purification step	volume (mL)	total protein (mg)[a]	total activity (μmol/min)[b]	specific activity (μmol min^{-1} mg^{-1})[b]	purification factor	% yield
cell lysate	26.0	235.94	2.63	0.0112	1.00	100
nickel-chelating Sepharose	6.7	76.94	1.88	0.0245	2.19	71
Sephacryl S-200	4.8	47.39	1.20	0.0255	2.28	46

[a] Determined by the Bradford assay (BSA as a standard). [b] Determined at 3 mM Dnp-AQALPETGEE-NH_2 and 2 mM pentaglycine.

monocytogenes EGD-e, *Bacillus subtilis* 168, *Clostridium acetobutylicum* ATCC824, and *E. coli* K12). The program *pfsearch* was used to scan the genomes using a modified version of the PROSITE profile PS50847 that was created from a multiple-sequence alignment of known sortase substrates. The profile searches for sequences containing an LPXTG motif followed by 10−15 hydrophobic amino acids, and finally a positively charged tail, by giving positive scores to sequences fitting this criterion. The profile was modified to include positive scores for the positions of Leu, Pro, and Gly to reflect the results of the substrate specificity analysis, and a *pfsearch* cutoff value of 4.5 was used. Sequences without a LPXTG tripartite motif followed by a hydrophobic domain and a positive charge were removed from consideration as possible substrates. The resulting list of genes was further refined to ensure that hits contained a putative sorting signal localized to the C-terminus of the protein product. Remaining hits were analyzed with the program SIGNALP (http://www.cbs.dtu.dk/services/signalp/) to verify that the proteins had been targeted for secretion (*23*−*25*). Finally, a Kyte−Doolittle hydropathy analysis was performed on each remaining protein to segregate putative cell surface-anchored substrates from integral membrane proteins (*26*). Sequences containing variants of the LPXTG motif were included in Table 3.

Cell Adhesion Assays. The ability of *S. aureus* to bind fibronectin was determined using a microtiter plate cell-based adhesion assay (*27*). Overnight cultures of *S. aureus* (Newman, SKM12, SKM7, and SKM14) were used to inoculate fresh tryptic soy broth (TSB), and were grown to mid-log phase (OD_{600} = 0.5). Fibronectin-coated flat-bottomed 96-well microtiter plates (Biocoat Cell Environments, Becton Dickenson Labware, Bedford, MA) were washed three times with PBS at room temperature (rt). An aliquot of the bacterial suspension (100 μL) was added to each well, and the plates were incubated at 37 °C for 2 h. The suspension was discarded, and the plates were washed three times with PBS. The cells were fixed by the addition of 2.0% (v/v) glutaraldehyde for 30 min. The bacteria were then washed with PBS; a crystal violet solution (25 g/L in distilled H_2O) was added, and the plates were incubated at room temperature for 15 min. The plates were then washed again with PBS and allowed to dry, and the absorbance at 570 nm was measured in a microtiter plate reader (Thermo Lab Systems Multiskan Spectrum).

Immunofluorescent Detection of Surface-Anchored Protein A. Bacterial cultures were grown to mid-log phase (OD_{600} = 0.3−0.6) in TSB medium. An aliquot of the culture suspension (1.5 mL) was centrifuged to pellet the bacteria (10 min at 8000*g* and 4 °C). Pellets were repetitively resuspended in PBS (1.0 mL), centrifuged three times, and finally resuspended in PBS (1.0 mL). The cell suspension (1.0 mL) was subsequently pipetted onto poly-L-lysine-coated glass slides and incubated at room temperature for 15 min to facilitate adsorption. Slides were washed with PBS (4 mL) three times, and excess PBS was pipetted off the slide. Slides were blocked with 4 mL of 2% (w/v) BSA in PBS at room temperature for 1 h, and washed three times with PBS (4 mL). Slides were incubated at room temperature for 1 h in the dark with 4 mL of Cy3-labeled IgG diluted 1:1000 (Jackson ImmunoResearch Laboratories, Inc., West Grove, PA) in 2% (w/v) BSA in 1× PBS and washed three times with PBS (4 mL). Excess PBS was removed, and a coverslip was placed over each slide. Slides were immediately viewed and photographed (λ_{ex} = 550 nm, λ_{em} = 565 nm) using an Eclipse E800 microscope (Nikon) equipped with a Sensicam camera (Cooke).

Transmission Electron Microscopy. S. aureus cells were grown in TSB medium to mid-log phase. An aliquot of the cell culture was removed (300 μL), pelleted, and subjected through 10 cycles of resuspension in water (1 mL) and centrifugation to remove media and excess buffer salts. The cells were resuspended in water (1 mL), and 5 μL of this suspension was deposited onto a Formar- and carbon-coated copper grid screen (200 mesh). Excess liquid was blotted away, and the grid was stained with 0.25% phosphotungstenic acid (5 μL, pH 7.4) for 30 s. The excess was removed by blotting, and the grid was allowed to air-dry. Transmission electron micrographs were obtained at a 50000× magnification level using a Joel 1010 electron microscope equipped with a digital imaging system.

RESULTS

Expression and Purification of Hexahistidine-Tagged S. aureus SrtA. The *S. aureus srtA* gene encodes a protein product of 206 amino acids containing a highly conserved TLXTC active site motif and a 24-amino acid N-terminal hydrophobic domain that facilitates membrane anchoring. Schneewind and co-workers previously demonstrated that deletion of this N-terminal sequence facilitates solubilization of the enzyme, with preservation of enzymatic activity (*15*, *28*). In an effort to generate high levels of soluble SrtA for activity and substrate specificity analyses, we prepared $SrtA_{\Delta N24}$ using pET vector-based expression construct (Novagen) containing the N-terminal 24-amino acid deletion as well as an N-terminal hexahistidine affinity tag. SrtA was efficiently overproduced in *E. coli* strain BL21(DE3) and purified to homogeneity using Ni(II)-chelate affinity chromatography and gel filtration (Figure 1). Purified SrtA was obtained (47 mg) after a 2.3-fold purification resulting in a 46% yield from 2 L of bacterial culture (Table 1). Enzyme purity was verified by SDS−PAGE analysis with Coomassie staining (Figure 1).

Analysis of Sortase SrtA Activity. Initial biochemical characterization of SrtA was performed using a fluorescence quenching *hydrolysis* assay utilizing either the chromophore-

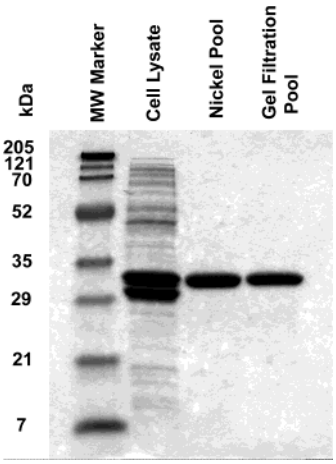

FIGURE 1: SDS−PAGE analysis depicting the purification of SrtA.

quencher pairs Dabcyl and Edans (Dabcyl-QALPETGEE-Edans) or Abz and Dnp [Abz-LPETG-Dap(Dnp)] (*29*, *30*). However, we recently showed that these assays are invalid for detailed kinetic investigations as they are subject to marked fluorescence inner filter effect quenching, resulting in prematurely hyperbolic *velocity* versus *substrate* profiles and erroneous representation of the true kinetic parameters k_{cat} and K_M (*31*). As a result, we developed a facile HPLC activity assay for SrtA *transpeptidation* activity that utilizes the substrates H-Gly_5-OH and Abz-LPETG-Dap(Dnp)-NH_2, producing Abz-LPETGGGGG-OH and NH_2-G-Dap(Dnp)-NH_2 (*31*). Using this assay, we determined that the k_{cat} is 0.27 s^{-1}, the K_M of Abz-LPETG-Dap(Dnp)-NH_2 is 5.5 mM, and the K_M of Gly_5 is 137 μM. These values represent a 300-fold increase in K_M for the LPXTG substrate, a 12000-fold increase in k_{cat}, and a 35-fold change in k_{cat}/K_M over previously reported values. Although SrtA clearly processed an LPXTG-containing substrate, at concentrations of up to 100 μM and reaction times of up to 360 min, it failed to catalyze both hydrolysis and transpeptidation reactions with peptides containing an inverted sorting signal motif [Abz-GTEPL-Dap(Dnp)-NH_2] or the putative SrtB isoform recognition motif NPQTN [as Abz-NPQTN-Dap(Dnp)-NH_2], as was anticipated (data not shown) (*14*).

Substrate Specificity Analysis of SrtA Using an LPXTG-Derived Peptide Library. We next examined the *in vitro* substrate specificity of $SrtA_{\Delta N24}$ for LPXTG and variants using a peptide library approach. In preparation for these studies, we synthesized Dnp-AQALPETGEE-NH_2 by solid-phase methods and confirmed its activity with $SrtA_{\Delta N24}$. Dnp was chosen as the sole chromophore to simplify the synthesis of the library. As shown in Figure 2, $SrtA_{\Delta N24}$ catalyzed the transpeptidation of this substrate with the following kinetic parameters: $k_{cat} = 0.013$ s^{-1} and $K_M = 5.6$ mM. While the k_{cat} is slightly lower than that found using the Abz-LPETG-Dap(Dnp)-NH_2 substrate, the K_M values are nearly identical, indicating that the Dnp-containing peptides could be used to probe substrate specificity.

With this information in hand, we constructed five 18-member peptide libraries on a 0.1 mmol scale by parallel synthesis, each library containing a single positional variant of the LPXTG sorting signal sequence. Cys and Trp residues were omitted from the library to simplify the library synthesis, as these residues are prone to oxidation. These libraries were subsequently assayed by HPLC for transpeptidation by $SrtA_{\Delta N24}$ under both initial rate conditions and extended incubation conditions to reveal substrate positional tolerances. The amount of product formed after 30 and 360 min was determined for each member of the library (Figures 3 and 4). At 30 min, the level of product formation was determined to be less than 10% for each library member as judged by quantitative HPLC analysis. Transpeptidation products from reaction mixtures containing Dnp-ALPHTG-NH_2, Dnp-ALPRTG-NH_2, and Dnp-ALPKTG-NH_2 coeluted with the starting material, although the concentrations of their respective transpeptidation products were estimated to lie

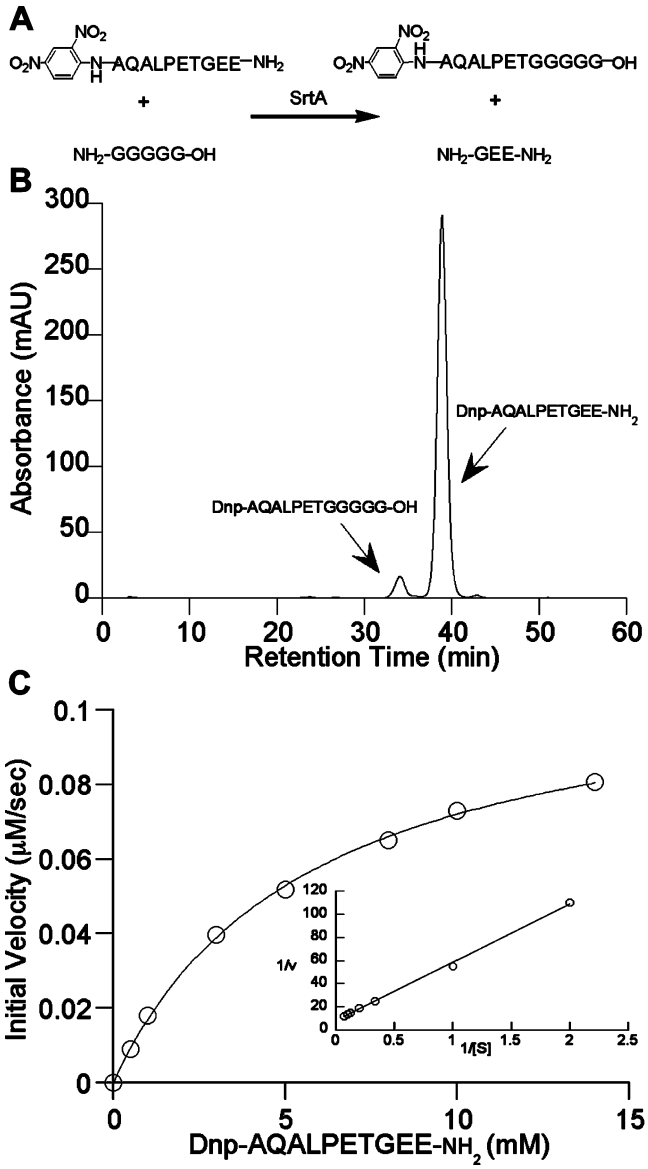

FIGURE 2: HPLC-based sortase assay using Dnp-AQALPETGEE-NH_2. (A) Sortase-catalyzed transpeptidation reaction of Dnp-AQALPETGEE-NH_2 and pentaglycine. (B) Representative HPLC trace showing the substrate Dnp-AQALPETGEE-NH_2 and the product Dnp-AQALPETGGGGG-OH. The chromatographic tracing corresponds to UV absorption at 355 nm of a 30 μL assay aliquot quenched with HCl after 30 min. Initial velocities were calculated from the linear portion of each assay, and the peak area was converted to concentration as described in Experimental Procedures. (C) Determination of K_M (Dnp-AQALPETGEE-NH_2) for $SrtA_{\Delta N24}$. Assays were performed at 37 °C in the presence of Gly_5 (2 mM), Dnp-AQALPETGEE-NH_2 (0−14 mM), and $SrtA_{\Delta N24}$ (8.4 μM). Estimates of the kinetic parameters ($K_M = 5.6$ mM and $k_{cat} = 0.013$ s^{-1}) were determined.

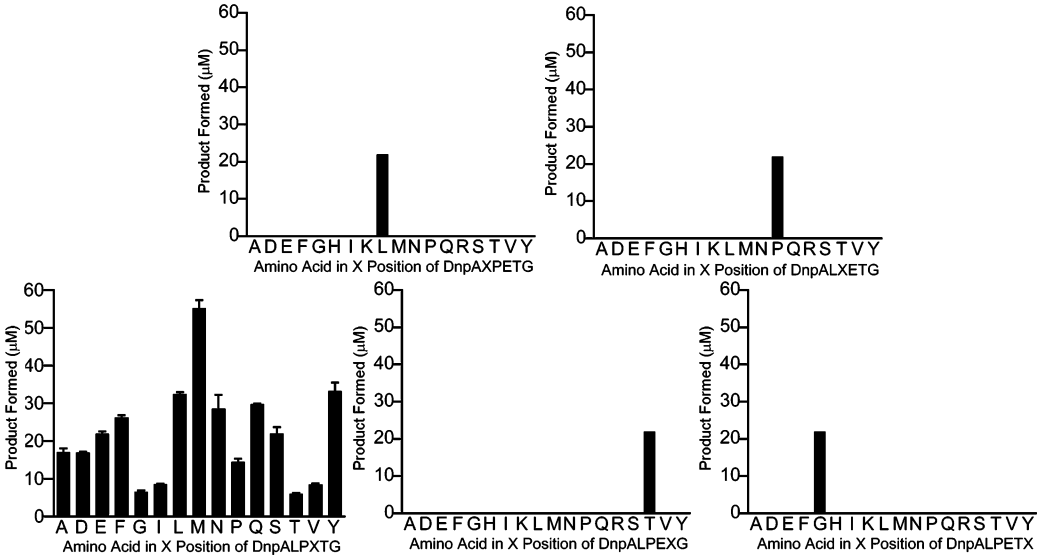

FIGURE 3: Initial velocity analysis of the sortase substrate library. Assays were performed in 100 μL reaction mixtures containing $SrtA_{\Delta N24}$ (15 μM), Gly_5 (2 mM), and peptide substrate (300 μM). Reactions were initiated by the addition of enzyme, mixtures incubated at 37 °C for 30 min, and then reactions quenched by the addition of 50 μL of 1 N HCl.

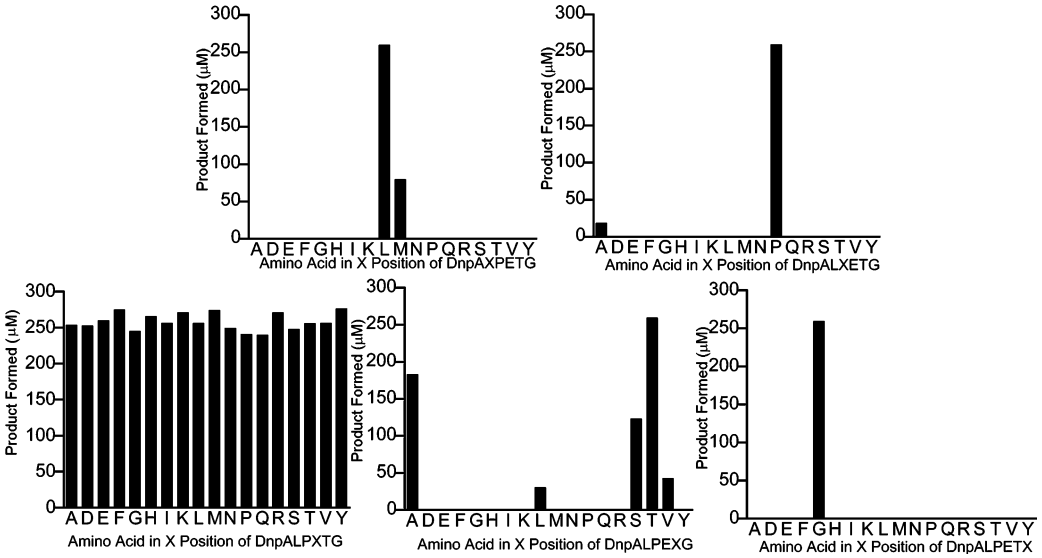

FIGURE 4: End point analysis of the sortase substrate library. Assays were performed in 100 μL reaction mixtures containing $SrtA_{\Delta N24}$ (60 μM), Gly_5 (2 mM), and peptide substrate (300 μM). Reactions were initiated by the addition of enzyme, mixtures incubated at 37 °C for 360 min, and then reactions quenched by the addition of 50 μL of 1 N HCl.

between 10 and 20 μM as judged by MALDI-TOF mass spectrometry (data not shown).

Under initial rate conditions (30 min, 15 μM enzyme), the kinetically preferred amino acids in positions 1, 2, 4, and 5 of the LPXTG motif were consensus residues Leu, Pro, Thr, and Gly, respectively, as shown in Figure 3. Surprisingly, no other residues were tolerated in these positions under the conditions that were examined. In position 3, where high residue variability has been observed in native sortase substrates, all 18 substitutions were tolerated. We observed a 10-fold variation between the best substrate (Dnp-ALPMTG-NH_2, 36.7 μM product formed) and the worst substrate (Dnp-ALPTTG-NH_2, 3.9 μM product formed). The prototypical substrate Dnp-ALPETG-NH_2, which mimics the sortase recognition motif of *S. aureus* protein A, was a moderate substrate for the enzyme where 14.5 μM product was observed to form in 30 min. SrtA exhibits a preference for Met, Tyr, Leu, Gln, and Asn at this position. β-Branched amino acids such as Ile, Val, and Thr are poorly tolerated. Neutral amino acids (Gln and Asn) are preferred over their charged counterparts (Glu and Asp). Collectively, these data indicate that the kinetically preferred substrate for SrtA exactly resembles the LPXTG consensus motif identified by sequence comparison of putative and experimentally verified sortase superfamily substrates from Gram-positive bacteria.

Two members of the library, Dnp-ALPETG-NH_2 and Dnp-ALPMTG-NH_2, were chosen for further comparative steady-state kinetic analyses. While the solubility limit of these peptides prevented complete enzyme saturation, initial velocity measurements were conducted at very low substrate concentrations relative to the estimated K_M ($<0.1K_M$). Under these conditions, the Michaelis−Menten equation simplifies to $v/[S] = V_{max}/K_M$, which provides a direct estimation of the enzyme's utilization ratio. Using this method, utilization ratios were calculated for Dnp-ALPMTG-NH_2 and Dnp-ALPETG-NH_2 and compared to those of Abz-LPETG-Dap-

Table 2: Kinetic Parameters of $SrtA_{\Delta N24}$

substrate	K_m (mM)	k_{cat} (s^{-1})	V_{max}/K_m (M^{-1} s^{-1})[a]
Abz-LPETG-Dap(Dnp)-NH_2	5.5	0.270	38.88
Dnp-AQALPETGEE-NH_2	5.6	0.013	2.00
Dnp-ALPETG-NH_2	ND[b]	ND[b]	3.43[c]
Dnp-ALPMTG-NH_2	ND[b]	ND[b]	8.83[c]

[a] V_{max}/K_m (utilization ratio) normalized by enzyme concentration where $V_{max}/K_m = v/[S]$ when $K_m \gg [S]$. [b] Not determined due to the inability to saturate enzyme within the substrate solubility limits. [c] Assays performed in 5% DMSO.

(Dnp)-NH_2 and Dnp-AQALPETGEE-NH_2 substrates, as summarized in Table 2.

Twenty-one genes encoding surface proteins belonging to the LPXTG family have been identified by *in silico* analysis of six *S. aureus* genome sequences (*32*). Of these, many contain the consensus LPXTG motif, while others contain positional variants, the most common being an Ala-to-Thr substitution in position 4 of the LPXTG sorting signal (e.g., SasF and SasD). To determine if SrtA is capable of catalyzing transpeptidation with noncanonical LPXTG variants, we examined SrtA for substrate promiscuity under extended reaction conditions. By extending the reaction time from 30 to 360 min and by increasing the enzyme concentration 4-fold to 60 μM, we showed additional members of the peptide library are substrates for $SrtA_{\Delta N24}$ (Figure 4). In position 1, Leu could be substituted with Met with modest efficiency, but intriguingly, other hydrophobes were not tolerated at this position. Likewise, the Pro residue in position 2 could be substituted with an Ala residue. As anticipated, all residues were similarly tolerated in the X variable position 3. In position 4 (Thr), the greatest positional variances were observed. In addition to threonine, SrtA processed substrates containing Ala, Ser, Val, or Leu at this position. No residues were tolerated as replacements for the Gly residue found in position 5.

Together, these results show that $SrtA_{\Delta N24}$ exhibits high selectivity for the Leu, Pro, Thr, and Gly residues found in the LPXTG consensus motif. These data also suggest that SrtA is capable of accepting substrates that contain point alterations of the LPXTG recognition motif, albeit at significantly reduced efficiency. Furthermore, the lack of cross talk observed from *in vitro* activity analysis of $SrtA_{\Delta N24}$ with a peptide containing the NPQTN SrtB recognition motif coupled with the prior observation of a lack of processing of LPXTG substrates *in vitro* and *in vivo* by SrtB (*14*) is strongly supportive of discreet roles for the two *S. aureus* sortase isoforms in protein anchoring. These findings are in excellent agreement with the prior *in vivo* characterization of SrtA and SrtB activity using reporter constructs composed of staphylococcal enterotoxin B (Seb) fusions to various substrate sorting signal sequences (*14*).

Electron Microscopy Reveals Differences in Cell Wall Structure in srtA$^-$ and srtB$^-$ Mutants. Our *in vitro* specificity studies strongly suggest that SrtA prefers to anchor LPXTG-containing but not NPQTN-containing proteins to the *S. aureus* cell surface. In contrast, SrtB appears to selectively prefer NPQTN-containing substrates. The *srtB* gene and the gene encoding its only known NPQTN substrate, *isdC*, are located within an operon whose expression is tightly regulated by environmental iron concentrations via the *fur* box promoter (*15*). SrtA, on the other hand, is under the control of a single promoter and is believed to anchor more than 20 different LPXTG-containing proteins, many of which are involved in facilitating adhesion, host colonization, and evasion of the host immune defenses (*14*, *32*). Because of the reduced level of SrtB expression in rich media (*15*), and the abundance of LPXTG-containing SrtA substrates that function by cell−cell or cell−protein contact, we predicted that inhibition of SrtA activity should significantly alter the thickness and morphology of the outer protein layer of the *S. aureus* cell wall.

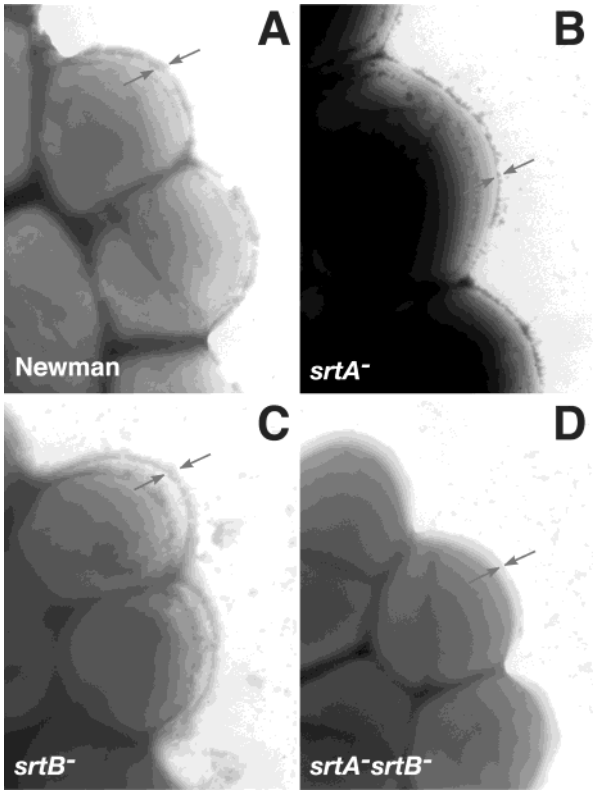

FIGURE 5: Electron micrographs of *S. aureus* showing the outer cell wall morphology in wild-type and sortase null mutant strains. Differences in the outer cell wall thickness and morphology of wild-type Newman, *srtA*$^-$, *srtB*$^-$, and *srtA*$^-$/*srtB*$^-$ *S. aureus* strains are highlighted with arrows.

We subsequently examined *S. aureus* Newman (wild type) and three sortase null mutant strains, *srtA*$^-$ (SKM 12), *srtB*$^-$ (SKM 7), and *srtA*$^-$/*srtB*$^-$ (SKM 14), by transmission electron microscopy (TEM) to visualize the outer cell wall morphology (*18*). As shown in Figure 5, TEM imaging of the *srtA*$^-$ mutant showed a dramatically thinned outer cell wall protein layer that was less than 25% as thick as that of the wild-type Newman strain as was anticipated due to the loss of surface proteins normally anchored by SrtA. However, the outer surface of the *srtB*$^-$ knockout strain appeared to be indistinguishable from that of the wild type. As anticipated, the *srtA*$^-$/*srtB*$^-$ double mutant contained a markedly thinned outer surface layer that appeared to be smoother than that of the *srtA*$^-$ mutant. Both *srtA*$^-$ and *srtA*$^-$/*srtB*$^-$ strains were significantly less clustered than either the Newman or *srtB*$^-$ strain (data not shown), suggesting that one or more surface proteins anchored by SrtA promoted cell−cell adhesion and colony formation. Collectively, these data strongly implicate SrtA as a major contributor to surface

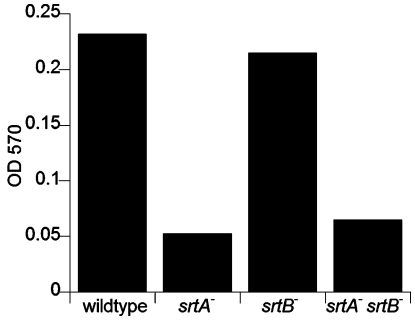

FIGURE 6: Fibronectin binding of *S. aureus* and mutants. Wild-type (Newman), *srtA*$^-$, *srtB*$^-$, and *srtA*$^-$/*srtB*$^-$ *S. aureus* were incubated on fibronectin-coated plates fixed with glutaraldehyde, washed, stained with crystal violet, and quantified by the absorbance at 570 nm.

protein attachment and outer surface morphology in *S. aureus*.

Detection of Surface-Anchored Proteins in srtA$^-$ *and srtB*$^-$ *Mutants.* Host colonization by *S. aureus* requires physical attachment to tissue. In *S. aureus*, sortase-anchored surface adhesins promote adhesion by binding to host extracellular matrix proteins. *S. aureus* FnbA and FnbB proteins bind human fibronectin and fibrinogen with nanomolar affinities, facilitating attachment to host endothelial tissue. To confirm that SrtA was responsible for anchoring these LPXTG-containing adhesions and to examine the potential for functional cross talk with SrtB, we monitored the ability of *S. aureus* Newman (wild type) and three sortase null mutant strains, *srtA*$^-$, *srtB*$^-$, and *srtA*$^-$/*srtB*$^-$ (*18*), to adhere to fibronectin-coated microtiter plates as a model for host tissue adhesion. As depicted in Figure 6, both wild-type and *srtB*$^-$ *S. aureus* strains adhered to the fibronectin-coated surfaces equally, indicating that these two strains possess a cell wall-anchored fibronectin-binding protein. In contrast, *srtA*$^-$ and *srtA*$^-$/*srtB*$^-$ strains exhibited a 5-fold decrease in the level of fibronectin binding, consistent with a significant reduction in the extent of surface anchoring of fibronectin-binding protein by SrtA.

Similarly, cell surface-anchored protein A, an LPXTG-containing protein, produced by *S. aureus* binds to the Fc region of human immunoglobulin IgG. Protein A has been implicated as a virulence factor (*33*), and binding to IgG is suspected to lead to opsonization and to contribute to the inhibition of phagocytosis. To confirm that SrtA and not SrtB is responsible for protein A anchoring, we monitored *S. aureus* Newman (wild type) and three sortase null mutant strains, *srtA*$^-$, *srtB*$^-$, and *srtA*$^-$/*srtB*$^-$ (*18*), for protein A display using immunofluorescence. We employed Cy3-labeled IgG as the fluorescent reporter molecule. As shown in Figure 7, *S. aureus* Newman and *srtB*$^-$ strains were intensely fluorescent and adhered strongly to the poly-L-lysine-coated glass slides. In contrast, SrtA deletion strains *srtA*$^-$ and *srtA*$^-$/*srtB*$^-$ were nearly devoid of fluorescence. Furthermore, cells adhered less to the slides, suggesting that SrtA deletion resulted in changes to cell surface protein composition and adhesion capacity. These immunofluorescence results, when taken together with the aforementioned cell adhesion assay results, clearly confirm that SrtA is responsible for anchoring these LPXTG-containing proteins. Furthermore, the preservation of protein A- and fibronectin binding protein-mediated surface attachment in the *srtB*$^-$ mutant suggests that little to no cross talk exists between the two isoforms. These data point to SrtA activity as a prime target for inhibition of *S. aureus* colonization.

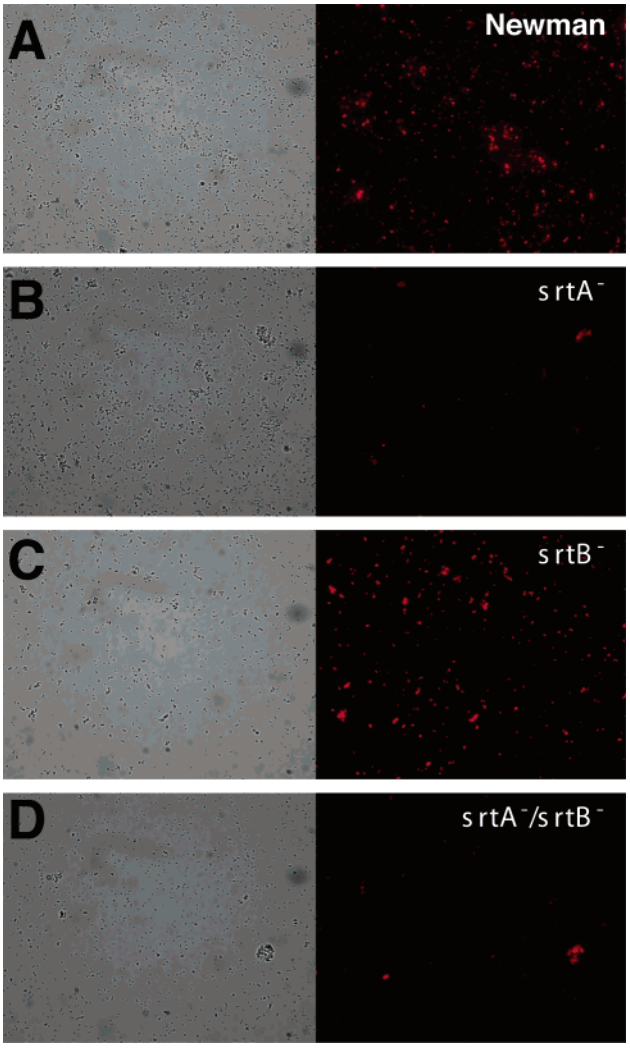

FIGURE 7: Immunofluorescent IgG binding of *S. aureus* and mutants. Bright field (left) and fluorescent (right) visualization of *S. aureus*. Fluorescently labeled IgG binds only when a functional protein A is displayed on the cell surface: (A) wild type, (B) *srtA*$^-$, (C) *srtB*$^-$, and (D) *srtA*$^-$/*srtB*$^-$ *S. aureus*.

DISCUSSION

The sudden rise in the number of clinical cases of antimicrobial resistance in Gram-positive human pathogens such as *S. aureus* and *Enterococcus faecium* has seriously impacted our ability to overcome opportunistic infectious disease. As strides are made in the generation of new antimicrobials to combat resistant phenotypes, increasing research efforts have been directed at understanding the underlying molecular mechanisms of microbial pathogenesis with the hope of exploiting critical processes that are essential for infection onset and propagation. Sortase activity has recently been identified as a key reaction that facilitates the subsequent adhesion, colonization, and surface presentation of virulence factors for numerous infectious diseases involving Gram-positive pathogens. As a result, this enzyme superfamily has emerged as an important target for the development of a new genre of antivirulence-based chemotherapeutic agents. Given the relatively large number of

Table 3: LPXTG Variant Sorting Signals in Select Gram-Positive Bacteria

modified position of the LPXTG motif	noncanonical sorting signal	protein identifier	species	ref
Leu	VPDTG	NID	*Streptococcus pneumoniae*	*7*
	IPQTG	NID	*St. pneumoniae*	*7*
	YPRTG	NID	*St. pneumoniae*	*7*
	SPKTG	NID	*C. difficile*	*7*
	FPKTG	EF0093	*E. faecalis* V583	this study, TIGR
	FPQTG	EF1896	*E. faecalis* V583	this study, TIGR
	FPQTG	EF2347	*E. faecalis* V583	this study, TIGR
	YPKTG	EF2505	*E. faecalis* V583	this study, TIGR
	IPKTG	lmo0435	*L. monocytogenes* egd-e	*16*
	IPALG	lmo1666	*L. monocytogenes* egd-e	*16*
Pro	LAASS	lmo0463	*L. monocytogenes* egd-e	*16*
	LADTG	EF0886	*E. faecalis* V583	this study, TIGR
	LAETG	CAB92248.1	*Str. coelicolor*	*7*
	LAETG	CAB69780.1	*Str. coelicolor*	*7*
	LAETG	CAA19902.1	*Str. coelicolor*	*7*
	LAATG	CAB82021.1	*Str. coelicolor*	*7*
	LAHTG	CAB92566.1	*Str. coelicolor*	*7*
	LASTG	CAB61716.1	*Str. coelicolor*	*7*
	LAETG	CAB50949.1	*Str. coelicolor*	*7*
	LAETG	CAB72217.1	*Str. coelicolor*	*7*
	LAETG	CAB61161.1	*Str. coelicolor*	*7*
	LASTG	6911555	*Arthrobacter* sp.	*7*
	LSRTG	477578	*Arthrobacter viscosus*	*7*
	LALTG	NID	*C. diphtheriae*	*7*
	LGNTG	NID	*C. diphtheriae*	*7*
	LAFTG	NID	*C. diphtheriae*	*7*
Thr	LPTAG	inlH	*L. monocytogenes* egd-e	*16*
	LPKAG	lmo0320	*L. monocytogenes* egd-e	*16*
	LAASS	lmo0463	*L. monocytogenes* egd-e	*16*
	LPISS	lmo0821	*L. monocytogenes* egd-e	this study, TIGR
	IPALG	lmo1666	*L. monocytogenes* egd-e	*16*
	LPAKT	CAC0403	*C. acetobutylicum* ATCC824	this study, TIGR
	LPKAN	EF1824	*E. faecalis* V583	this study, TIGR
	LPAAG	SasD	*S. aureus* COL	*1*
	LPKAG	SasF	*S. aureus* COL	*1*
	LPLSG	AAB57674	*A. naeslundii*	*12*
	LPKAG	S54396	*P. magnus*	*35*
				36
	LPEAG	CAA54857	*P. magnus*	*37*
	LPAAG	CAA80122	*S. agalactiae*	*38*
Gly	LPKTS	inlG	*L. monocytogenes* egd-e	*16*
	LAASS	lmo0463	*L. monocytogenes* egd-e	*16*
	LPISS	lmo0821	*L. monocytogenes* egd-e	this study, TIGR
	LPDTA	yfkN	*B. subtilis* 168	*7*
	LPDTS	yhcR	*B. subtilis* 168	this study, TIGR
	LPAKT	CAC0403	*C. acetobutylicum* ATCC 824	this study, TIGR
	LPKTN	EF1092	*E. faecalis* V583	this study, TIGR
	LPKAN	EF1824	*E. faecalis* V583	this study, TIGR
	LPNTN	EF2525	*E. faecalis* V583	this study, TIGR
	LPNTA	NID	*B. anthracis*	*6*
	LPKTA	AAA25248	*Listeria paracasei*	*39*
	LPTTN	A35006	*St. pyogenes*	*40*
	LPTTN	AAF06282	*S. agalactiae*	*41*
	LPQTS	NID	*S. putrefasciens*	

sortase orthologs and potential substrates among Gram-positive pathogens, understanding the sortase specificity code will facilitate the identification of enzyme pathogenesis pairing that is essential for promoting the development of antivirulence chemotherapies for these infections. In this study, we have taken steps toward understanding the substrate specificity and physiological functions of *S. aureus* SrtA and SrtB isoforms.

Fischetti and Schneewind previously showed that the LPXTG consensus pentapeptide C-terminal motif was necessary and sufficient for directing proper sorting of proteins of Gram-positive cocci (*10*). We showed that peptides containing the LPXTG motif were indeed kinetically favored as substrates over all positional variants of this sequence when examined under initial rate conditions. Furthermore, our data reflect the capacity of SrtA to process noncanonical LPXTG variants that mimic natively occurring sortase substrates *in vivo*, such as SasD (LPAAG) and SasF (LPKAG). As these variations appear to occur in *S. aureus* sortase substrates in discreet positions, for insight into whether LPXTG sequence variations track to specific positions, we examined the sortase substrates from eight different Gram-positive bacterial genomes using a modification of the tripartite search motif algorithm developed by Masmussen

(*11*). Indeed, the positional variant consensus sequence of SrtA observed *in vitro* (M-A-X-A/S/V/L-G) was qualitatively similar to the U-A-X-A/S-N/S/A (where U is a hydrophobe) consensus sequence obtained by from *in silico* analysis (Table 3). Although it is premature to conclude that we have uncovered a substrate specificity determinant, it is intriguing that the differences between the NPQTN and LPXTG recognition motifs occur at positions 1 and 5. Perhaps SrtB may exhibit a different positional specificity than SrtA for these positions. Taken together, these data highlight the potential for using peptide libraries to reveal specificity determinants for sortase superfamily isoforms. Future use of positional scanning peptide libraries, potentially facilitated by a recently described fluorescence resonance energy transfer assay for sortase activity (*34*), will facilitate sortase specificity analysis when the substrates have not yet been identified via genetic, genomic, or biochemical means.

We have confirmed that SrtA and SrtB possess distinct physiological roles. Three independent *in vivo* methods confirmed that SrtA is responsible for the display of important virulence factors in *S. aureus*. Using cell-based adhesion assays and protein A immunofluorescence assays, we have shown that SrtA but not SrtB is responsible for the anchoring of fibronectin binding protein and protein A. We have also shown by electron microscopy that *srtA* mutants have significantly altered cell wall morphologies while *srtB* mutants appear to be identical to the wild type. These data reflect the apparent lack of cross-substrate specificity between the two isoforms *in vitro* and with the anchoring of full-length virulence-associated proteins *in vivo*. These data are in excellent agreement with prior *in vivo* reporter gene studies in *S. aureus* and results from analysis of infection propagation and virulence in murine models of septic arthritis using *srtA* and *srtB* deficient *S. aureus* strains (*14*, *18*). As SrtA is responsible for anchoring the majority of staphylococcal proteins involved in virulence, adhesion, and colonization, we are hopeful that inhibitors of SrtA function will translate into antivirulence chemotherapeutics for staphylococcal infections, especially from those resistant to front line antibiotics such as methicillin or vancomycin.

ACKNOWLEDGMENT

We thank Prof. Olaf Schneewind and Adrienne Perry for the kind gift of *srtA*$^-$, *srtB*$^-$, and *srtA*$^-$/*srtB*$^-$ *S. aureus* knockout strains. We also acknowledge Prof. William DeGrado for access to their peptide synthesis instrumentation and mass spectrometer. We thank Dr. Neelima Shah for assistance with electron microscopy experiments.

REFERENCES

1. Mazmanian, S. K., Ton-That, H., and Schneewind, O. (2001) Sortase-catalysed anchoring of surface proteins to the cell wall of *Staphylococcus aureus*, *Mol. Microbiol. 40*, 1049−1057.
2. Navarre, W. W., and Schneewind, O. (1999) Surface proteins of Gram-positive bacteria and mechanisms of their targeting to the cell wall envelope, *Microbiol. Mol. Biol. Rev. 63*, 174−229.
3. Mazmanian, S. K., Liu, G., Jensen, E. R., Lenoy, E., and Schneewind, O. (2000) *Staphylococcus aureus* sortase mutants defective in the display of surface proteins and in the pathogenesis of animal infections, *Proc. Natl. Acad. Sci. U.S.A. 97*, 5510−5515.
4. Bolken, T. C., Franke, C. A., Jones, K. F., Zeller, G. O., Jones, C. H., Dutton, E. K., and Hruby, D. E. (2001) Inactivation of the *srtA* gene in *Streptococcus gordonii* inhibits cell wall anchoring of surface proteins and decreases *in vitro* and *in vivo* adhesion, *Infect. Immun. 69*, 75−80.
5. Garandeau, C., Reglier-Poupet, H., Dubail, I., Beretti, J. L., Berche, P., and Charbit, A. (2002) The sortase SrtA of *Listeria monocytogenes* is involved in processing of internalin and in virulence, *Infect. Immun. 70*, 1382−1390.
6. Bierne, H., Mazmanian, S. K., Trost, M., Pucciarelli, M. G., Liu, G., Dehoux, P., Jansch, L., Garcia-del Portillo, F., Schneewind, O., and Cossart, P. (2002) Inactivation of the *srtA* gene in *Listeria monocytogenes* inhibits anchoring of surface proteins and affects virulence, *Mol. Microbiol. 43*, 869−881.
7. Pallen, M. J., Lam, A. C., Antonio, M., and Dunbar, K. (2001) An embarrassment of sortases: a richness of substrates? *Trends Microbiol. 9*, 97−102.
8. Barnett, T. C., and Scott, J. R. (2002) Differential recognition of surface proteins in *Streptococcus pyogenes* by two sortase gene homologs, *J. Bacteriol. 184*, 2181−2191.
9. Osaki, M., Takamatsu, D., Shimoji, Y., and Sekizaki, T. (2003) Allelic variation in *srtA*s of *Streptococcus suis* strains, *FEMS Microbiol. Lett. 219*, 195−201.
10. Fischetti, V. A., Pancholi, V., and Schneewind, O. (1990) Conservation of a hexapeptide sequence in the anchor region of surface proteins from Gram-positive cocci, *Mol. Microbiol. 4*, 1603−1605.
11. Janulczyk, R., and Rasmussen, M. (2001) Improved pattern for genome-based screening identifies novel cell wall-attached proteins in Gram-positive bacteria, *Infect. Immun. 69*, 4019−4026.
12. Perry, A. M., Ton-That, H., Mazmanian, S. K., and Schneewind, O. (2002). Anchoring of surface proteins to the cell wall of *Staphylococcus aureus*. III. Lipid II is an *in vivo* peptidoglycan substrate for sortase-catalyzed surface protein anchoring, *J. Biol. Chem. 277*, 16241−16248.
13. Ruzin, A., Severin, A., Ritacco, F., Tabei, K., Singh, G., Bradford, P. A., Siegel, M. M., Projan, S. J., and Shlaes, D. M. (2002) Further evidence that a cell wall precursor [C(55)-MurNAc-(peptide)-GlcNAc] serves as an acceptor in a sorting reaction, *J. Bacteriol. 184*, 2141−2147.
14. Mazmanian, S. K., Ton-That, H., Su, K., and Schneewind, O. (2002) An iron-regulated sortase anchors a class of surface protein during *Staphylococcus aureus* pathogenesis, *Proc. Natl. Acad. Sci. U.S.A. 99*, 2293−2298.
15. Mazmanian, S. K., Skaar, E. P., Gaspar, A. H., Humayun, M., Gornicki, P., Jelenska, J., Joachmiak, A., Missiakas, D. M., and Schneewind, O. (2003) Passage of heme-iron across the envelope of *Staphylococcus aureus*, *Science 299*, 906−909.
16. Cabanes, D., Dehoux, P., Dussurget, O., Frangeul, L., and Cossart, P. (2002) Surface proteins and the pathogenic potential of *Listeria monocytogenes*, *Trends Microbiol. 10*, 238−245.
17. Mazmanian, S. K., and Schneewind, O. (2002) Cell wall-anchored surface proteins and lipoproteins of Gram-positive bacteria, in *Bacillus subtilis and its closest relatives: From genes to cells* (Sonenshein, A. L., Hoch, J. A., and Losick, R., Eds.) pp 57−70, ASM Press, Washington, DC.
18. Jonsson, I. M., Mazmanian, S. K., Schneewind, O., Bremell, T., and Tarkowski, A. (2003) The role of *Staphylococcus aureus* sortase A and sortase B in murine arthritis, *Microbes Infect. 5*, 775−780.
19. Sambrook, J., Fritsch, E. F., and Maniatis, T., Eds. (1989) *Molecular cloning: A laboratory manual*, 2nd ed., Cold Spring Harbor Laboratory Press, Plainview, NY.
20. Pace, C. N., Vajdos, F., Fee, L., Grimsley, G., and Gray, T. (1995) How to measure and predict the molar absorption coefficient of a protein, *Protein Sci. 4*, 2411−2423.
21. Gill, S. C., and von Hippel, P. H. (1989) Calculation of protein extinction coefficients from amino acid sequence data, *Anal. Biochem. 182*, 319−326.
22. Bradford, M. M. (1976) A rapid and sensitive method for the quantitation of microgram quantities of protein utilizing the principle of protein-dye binding, *Anal. Biochem. 72*, 248−254.
23. Nielsen, H., Engelbrecht, J., Brunak, S., and von Heijne, G. (1997) A neural network method for identification of prokaryotic and eukaryotic signal peptides and prediction of their cleavage sites, *Int. J. Neural Syst. 8*, 581−599.
24. Nielsen, H., Engelbrecht, J., Brunak, S., and von Heijne, G. (1997) Identification of prokaryotic and eukaryotic signal peptides and prediction of their cleavage sites, *Protein Eng. 10*, 1−6.
25. Nielsen, H., Brunak, S., and von Heijne, G. (1999) Machine learning approaches for the prediction of signal peptides and other protein sorting signals, *Protein Eng. 12*, 3−9.

26. Kyte, J., and Doolittle, R. F. (1982) A simple method for displaying the hydropathic character of a protein, *J. Mol. Biol. 157*, 105−132.
27. Elgalai, I., and Foster, H. A. (2003) Comparison of adhesion of wound isolates of *Staphylococcus aureus* to immobilized proteins, *J. Appl. Microbiol. 94*, 413−420.
28. Ton-That, H., Liu, G., Mazmanian, S. K., Faull, K. F., and Schneewind, O. (1999) Purification and characterization of sortase, the transpeptidase that cleaves surface proteins of *Staphylococcus aureus* at the LPXTG motif, *Proc. Natl. Acad. Sci. U.S.A. 96*, 12424−12429.
29. Ton-That, H., Mazmanian, S. K., Faull, K. F., and Schneewind, O. (2000) Anchoring of surface proteins to the cell wall of *Staphylococcus aureus*. Sortase catalyzed in vitro transpeptidation reaction using LPXTG peptide and NH(2)-Gly(3) substrates, *J. Biol. Chem. 275*, 9876−9881.
30. Ilangovan, U., Ton-That, H., Iwahara, J., Schneewind, O., and Clubb, R. T. (2001) Structure of sortase, the transpeptidase that anchors proteins to the cell wall of *Staphylococcus aureus*, *Proc. Natl. Acad. Sci. U.S.A. 98*, 6056−6061.
31. Kruger, R. G., Dostal, P., and McCafferty, D. G. (2003) Development of an HPLC assay and revision of kinetic parameters for the *Staphylococcus aureus* sortase transpeptidase SrtA, *Anal. Biochem*. (in press).
32. Roche, F. M., Massey, R., Peacock, S. J., Day, N. P., Visai, L., Speziale, P., Lam, A., Pallen, M., and Foster, T. J. (2003) Characterization of novel LPXTG-containing proteins of *Staphylococcus aureus* identified from genome sequences, *Microbiology 149*, 643−654.
33. Palmqvist, N., Foster, T., Tarkowski, A., and Josefsson, E. (2002) Protein A is a virulence factor in *Staphylococcus aureus* arthritis and septic death, *Microb. Pathog. 33*, 239−249.
34. Kruger, R. G., Dostal, P., and McCafferty, D. G. (2002) An economical and preparative orthogonal solid-phase synthesis of fluorescein and rhodamine derivatized peptides: FRET substrates for the *Staphylococcus aureus* sortase SrtA transpeptidase reaction, *Chem. Commun.*, 2092−2093.
35. Kastern, W., Holst, E., Nielsen, E., Sjobring, U., and Bjorck, L. (1990) Protein L, a bacterial immunoglobulin-binding protein and possible virulence determinant, *Infect. Immun. 58*, 1217−1222.
36. Murphy, J. P., Trowern, A. R., and Duggleby, C. J. (1994) Nucleotide sequence of the gene for peptostreptococcal protein L, *DNA Sequence 4*, 259−265.
37. de Chateau, M., and Bjorck, L. (1996) Identification of interdomain sequences promoting the intronless evolution of a bacterial protein family, *Proc. Natl. Acad. Sci. U.S.A. 93*, 8490−8495.
38. Lindgren, P. E., McGavin, M. J., Signas, C., Guss, B., Gurusiddappa, S., Hook, M., and Lindberg, M. (1993) Two different genes coding for fibronectin-binding proteins from *Streptococcus dysgalactiae*. The complete nucleotide sequences and characterization of the binding domains, *Eur. J. Biochem. 214*, 819−827.
39. Holck, A., and Naes, H. (1992) Cloning, sequencing and expression of the gene encoding the cell-envelope-associated proteinase from *Lactobacillus paracasei* subsp. paracasei NCDO 151, *J. Gen. Microbiol. 138*, 1353−1364.
40. Chen, C. C., and Cleary, P. P. (1990) Complete nucleotide sequence of the streptococcal C5a peptidase gene of *Streptococcus pyogenes*, *J. Biol. Chem. 265*, 3161−3167.
41. Chmouryguina, I., Suvorov, A., Ferrieri, P., and Cleary, P. P. (1996) Conservation of the C5a peptidase genes in group A and B streptococci, *Infect. Immun. 64*, 2387−2390.

BI035920J